REPRESENTING AND ANALYSING THE KINEMATIC ROBUSTNESS OF ROBOTIC PLANETARY SYSTEMS

Dr. J. Hobbs [(1)], Dr. J. Rooney [(2)]

[(1)] JDH Innovation, 19 Charlcombe Rise, Portishead,
Bristol BS20 8NB, United Kingdom
e-mail: jd.hobbs@btinternet.com

[(2)] Faculty of Mathematics, Computing and Technology, The Open University,
Milton Keynes, MK7 6AA, United Kingdom
e-mail: j.rooney@open.ac.uk

ABSTRACT

This paper describes research into the kinematic robustness of autonomous robotic systems. Kinematic structures typical of those employed in the manipulation and locomotion elements of planetary exploration vehicles are represented using Graph Theory techniques, extended by the novel concept of the *Constraints Matrix*. This replaces the elements (zeroes and ones) of the standard adjacency matrix of the interchange graph of a kinematic system by integer elements representing the numbers of constrained degrees of freedom (dof) throughout the system. It is shown that, as motion faults develop progressively within a particular kinematic system, the succession of kinematic states lies along a trajectory in an abstract kinematic fault space derived from Constraints Matrix eigenvalues. For a 3-link system, progressing along the trajectory, the change from one kinematic state to the next is accompanied by a rotation of the corresponding (Constraints Matrix) orthonormal eigenvectors, according to the nature of each fault that has occurred. Thus, aspects of the robustness to, and recovery from kinematic faults, of a kinematic system are represented in geometrical terms.

MODELLING OF KINEMATIC SYSTEMS USING GRAPH THEORY

Kinematic topology refers to the organisational arrangement, juxtaposition and interconnection of components and sub-systems that involve movement. This provides a means whereby the manipulation and locomotion elements of planetary exploration vehicles and their subsystems can be represented, modelled and eventually designed, and Graph Theory [6] is one of several possible techniques for achieving this. Graph Theory is not discussed in detail here, although, for convenience, some relevant terms are defined within the text.

The first step in applying graph theory to a moving system is to identify the **kinematic chain** of, for example, a locomotion subsystem. The next step is then to generate the **interchange graph** representation of the kinematic chain, in which the links and joints of the chain are represented by vertices and edges respectively [2].

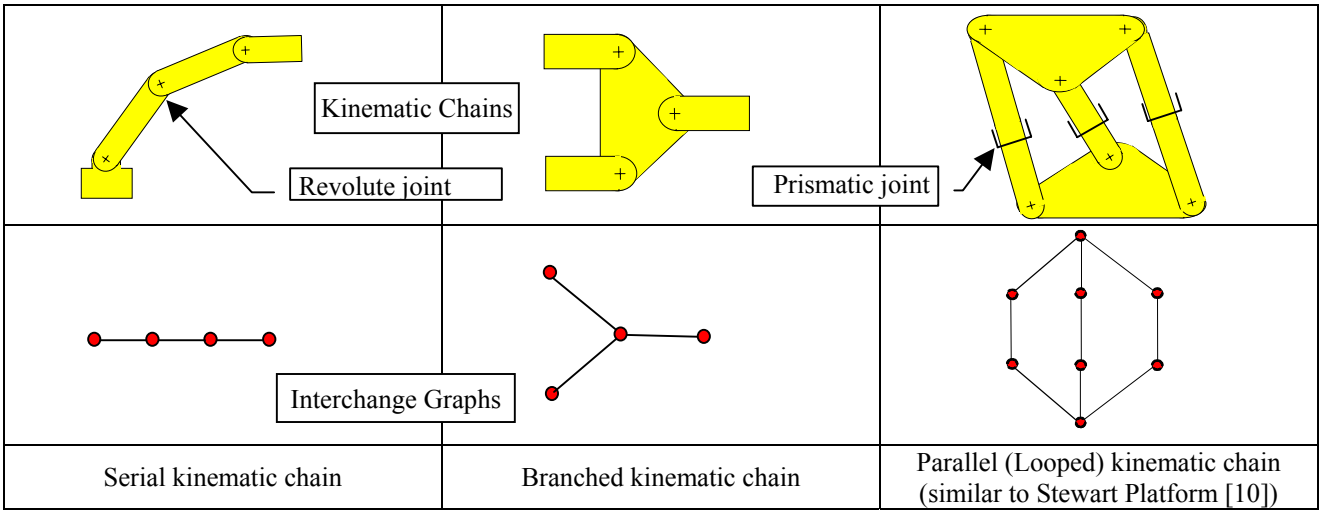

Fig.1: Kinematic Chains and Interchange Graphs of three 3-dof Manipulation/Locomotion systems

Fig.1 illustrates the kinematic chains of three 3-dof manipulation / locomotion systems - a serial kinematic chain (typically a robot manipulator), a branched kinematic chain (typically a legged locomotion system), and a parallel (looped) kinematic chain (typically a flight simulator platform), together with their interchange graphs.

The standard interchange graph representation of a kinematic system can yield insights into the system's kinematic structure and behaviour. However, its usefulness is limited by the fact that it does not directly represent some critical design features. Nor does it completely represent some functioning aspects such as the nature and operational status of the joints present, and whether or not these are active (driven or not), or passive. Therefore, the standard interchange graph representation is extended here to encompass the more general concept of the **kinematic state graph**. In this, each of the joints connecting a pair of links (graph vertices) is represented by a number of edges corresponding to the number of dof of that particular joint.

Franz Reuleaux (1829– 1905) defined six fundamental types of surface-contact joints between rigid bodies, the so-called 'lower kinematic pairs' [3][4], having dofs ranging from 1 to 3 – Table 1.

Table 1: The Six Reuleaux Surface-Contact 'Lower Kinematic Pairs'

Reuleaux Joint Type	**Revolute**	**Prismatic**	**Screw (helical)**	**Cylindric**	**Spherical**	**Planar**
Joint Symbol	R	P	H	C	S	E
Number of dof	1	1	1	2	3	3

Kinematic state graphs are illustrated in Figure 2, for three example systems each consisting of three links connected serially by two Reuleaux joints of various dofs. Note that a planar joint can be regarded as a serial combination of two non-parallel prismatic joints together with a revolute joint whose axis is orthogonal to the two prismatics (E ≡ R + 2P). Similarly, a spherical joint can be regarded as a serial combination of three revolute joints, where the three revolute axes all intersect at the same point (S ≡ 3R). Hence, with this viewpoint, all three dofs of a planar or spherical joint are controllable, and consequently we consider it possible for a particular E or S joint to lose one or more dofs in such a way that the remaining dofs are still controllable.

In this paper, the kinematic states of serial 3-link systems such as those shown in Fig.2 are denoted using the format (*l*,*r*) where *l* and *r* are respectively the numbers of dof in the left and right joints on either side of the central vertex (link). This format is readily extendable to larger serial kinematic systems consisting of more than three links and two joints.

When a degree of freedom of a joint is lost through a kinematic fault or failure, this is represented in the graph by replacing a full edge with a dashed edge – Fig.3. Additionally, where a joint is being actively driven, the edge is annotated '$(d)_{on}$'. Where a driven joint exists, but is inactive (by choice, or through a fault), this is shown as '$(d)_{off}$'.

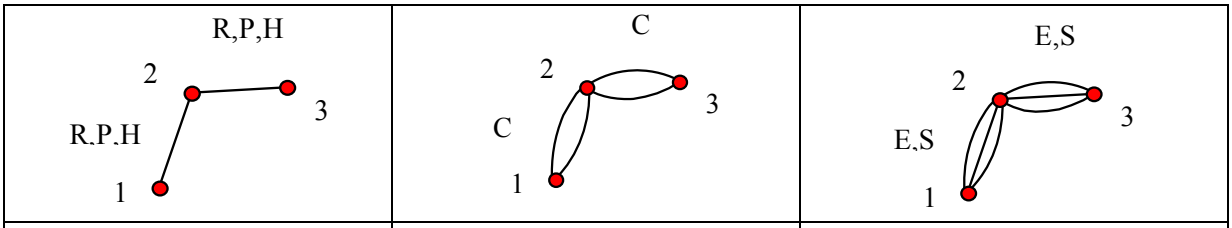

3- Link system (1,1) with two 1-dof joints - revolute, prismatic or screw. | *3- Link system (2,2) with two, 2-dof joints - cylindric.* | *3- Link system (3,3) with two 3-dof joints - planar or spherical.*

Fig.2: Kinematic State Graphs for Different Joint Types

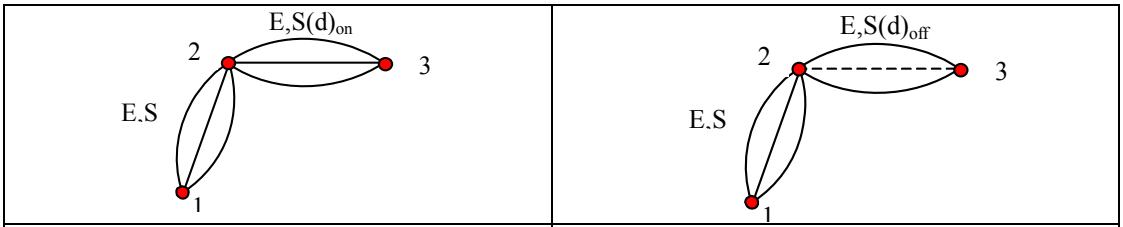

3-Link system (3,3) with two 3-dof joints - planar or spherical – with identification of active driven joint | *3-Link system (3,2) with two 3-dof joints - planar or spherical - driven joint, with 1 dof switched off or failed*

Fig.3: Kinematic State Graphs showing the Representation of Failed dof and Driven Joints

Thus, using this kinematic state graph representation, it is possible to represent many of the kinematic fault states of a system. It should be noted that, when representing joints by multiple edges in system fault states, two possible conditions arise. The first condition refers to those situations, where either the loss of one or more of the multiple edges connecting a particular pair of vertices is reversible, (e.g. caused by a motor switching on or off), or where, because of a fault or failure, the loss of only one of the several edges in a multiple edge between a pair of vertices has occurred. Here, some relative motion of the two links represented by the vertices in question remains possible, although the number of dof has been reduced. This case is referred to as being *'without total loss of edge'*. In this case, the graph retains the original number of vertices. The second instance refers to those situations where the change (again caused by a fault or failure) is irreversible and leads to the two links represented by the two vertices in question becoming locked together – in effect becoming the same link (vertex)– so that there is no relative motion between the two links concerned. This case is referred to as *'vertex identification with total loss of edge'*.

LINEAR ALGEBRA AND GRAPH REPRESENTATIONS

It is possible to develop graph representations using aspects of linear algebra to provide further insights into kinematic behaviour. The following definitions from linear algebra form the starting point:

The **Adjacency Matrix** of a graph (such as an Interchange Graph) with n vertices is defined as the square real symmetric $n \times n$ matrix $\mathbf{A}$ whose ij-th term is the number of edges joining vertex i and vertex j [6].

The **Characteristic Polynomial**, $P(\lambda)$, of a square matrix (such as an Adjacency Matrix) $\mathbf{A}$ is defined as the determinant $|\lambda\mathbf{I} - \mathbf{A}|$, where λ is a dummy variable, and $\mathbf{I}$ is a unit matrix of the same order as $\mathbf{A}$ [7].

The novel concept of a **Constraints Matrix**, **C** is introduced here to replace the zeroes and ones of the standard adjacency matrix of the interchange graph of a kinematic system by integers representing the number of constraints on each joint. In this representation, diagonal elements are no longer 'zeroes' but now become 'sixes', since no link (vertex) can have any degrees of freedom relative to itself. Those matrix elements representing edges connecting vertices between which no connections exist continue to be represented as zeroes.

Thus, for the nominal state of the 3-link (3,3) system with two 3-dof joints shown at the right-hand side of Fig.2:

$$\begin{bmatrix} 0 & 1 & 0 \\ 1 & 0 & 1 \\ 0 & 1 & 0 \end{bmatrix} \qquad \begin{bmatrix} 6 & 3 & 0 \\ 3 & 6 & 3 \\ 0 & 3 & 6 \end{bmatrix}$$

Adjacency Matrix Constraints Matrix

Fig.4: Adjacency and Constraints Matrices of a Typical 3-Link Serial Kinematic System (3,3) connected by Two 3-dof Joints

For the Constraints Matrix, the characteristic polynomial, $P(\lambda)$, is defined as the determinant:

$$P(\lambda) = |\lambda\mathbf{I} - \mathbf{C}| \quad \text{……………………………………………………} \quad (1)$$

Where **C** is the Constraints Matrix, and other symbols are as previously defined.

The eigenvalues, which are the roots of the characteristic polynomial, $P(\lambda)$, and their associated eigenvectors, which are the corresponding solutions for **X** of the equation:

$$\lambda\mathbf{X} = \mathbf{C}\mathbf{X} \quad \text{……………………………………………………} \quad (2)$$

can be evaluated from (1) by standard means [1][5]. For the example Constraints Matrix shown in Fig.4, the eigenvalues and eigenvectors are:

$$\text{eigenvalues} = \begin{bmatrix} 6 \\ 10.243 \\ 1.757 \end{bmatrix}, \qquad \text{eigenvectors} = \begin{bmatrix} 0.707 \\ 0 \\ -0.707 \end{bmatrix}, \begin{bmatrix} 0.5 \\ 0.707 \\ 0.5 \end{bmatrix}, \begin{bmatrix} 0.5 \\ -0.707 \\ 0.5 \end{bmatrix}$$

We now investigate whether constraints matrices can be used to characterise both the behaviour of kinematic systems in their nominal (unfailed) and failed states, and the transitions between these. In order to progress we consider in greater detail the nature of these transitions and the kinematic states connected by them. Together, these form a kinematic 'fault path' representing a system's response to a particular sequence of kinematic faults.

KINEMATIC FAULT PATHS

A kinematic fault path comprises a sequence of discrete steps between the kinematic states of a kinematic system, where each step corresponds to the loss of a degree of freedom within one of the joints of the system. Typically such a fault path continues through a number of intermediate kinematic states until a state is reached which represents a terminating kinematic state. Such a terminating state would be one where all system movement has been lost, or where the movement that remains cannot be utilised in any meaningful way. The number of sequences in which successive faults can occur grows rapidly with the number of joints in the system, and even for 'small' systems the number of permutations of fault occurrence is significantly high. Consider Fig.5, which identifies the kinematic states corresponding to faults in the 3-link (3,3) system shown on the right of Fig.2. For simplicity, here the sequence of faults develops in just one joint.

For ease of visualisation, the faults are considered to arise in discrete steps, although, in practice, this may not be the case, or the steps may follow one another so rapidly that effectively they are simultaneous. Successive fault states are numbered sequentially, with State 1 being taken as the nominal condition.

The degradation of an n-link kinematic system under the action of progressive faults may be visualised n-dimensionally. For a 3-link kinematic system, such as that in Fig.5, the constraints matrix is a 3×3 matrix and this has three eigenvalues, λ_1, λ_2, λ_3. These eigenvalues may be considered to be the three co-ordinates, (λ_1, λ_2, λ_3), of a point in a 3-dimensional eigenvalue space. As each fault occurs, the Constraints Matrix changes and so, therefore, do its three eigenvalues. A sequence of faults produces a 'fault trajectory' within the (eigenvalue) space. Fig.6 attempts to show this for the three-dimensional eigenvalue space in which the four points representing States 1, 2, 3, and 4 of the 3-link (3,3) kinematic system shown in Fig.5 are embedded.

ROTATION OF EIGENVECTORS

As a kinematic system progresses through a sequence of kinematic fault states, the latter give rise to a corresponding sequence of Constraints Matrices (one for each step of the sequence). Because the latter are (real) symmetric matrices, their eigenvectors are orthogonal, and additionally, these are usually normalised since, by convention, only eigenvector direction is of relevance.

Fig.7 shows an example of the behaviour of the orthonormal eigenvectors corresponding to the Constraints Matrices, as the fault path illustrated in Fig.5 is traversed. Essentially the effect of each system fault is to cause a rotation of the triad of eigenvectors, considered as a rigid frame forming a rigid body. For a higher order system (such as an n-link system under the action of successive faults), the triad of eigenvectors would be replaced with a 'rigid' orthonormal system (an 'n-ad') of n eigenvectors.

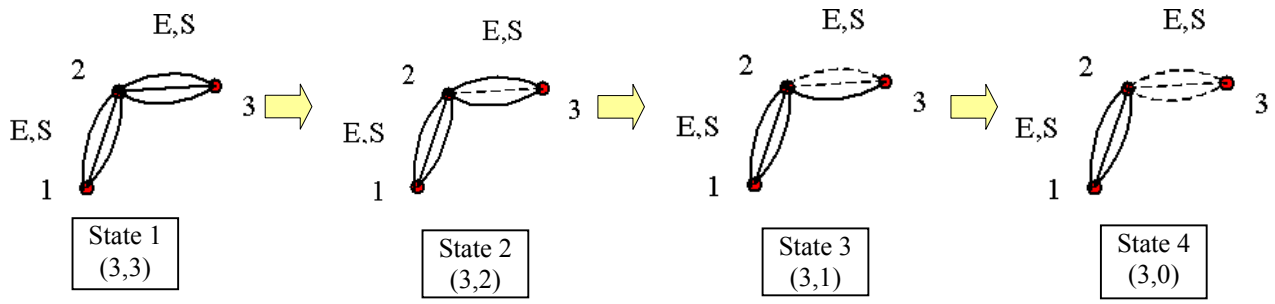

Fig.5: Degeneration of a 3-Link (3,3) System under the action of Progressive Faults in one joint

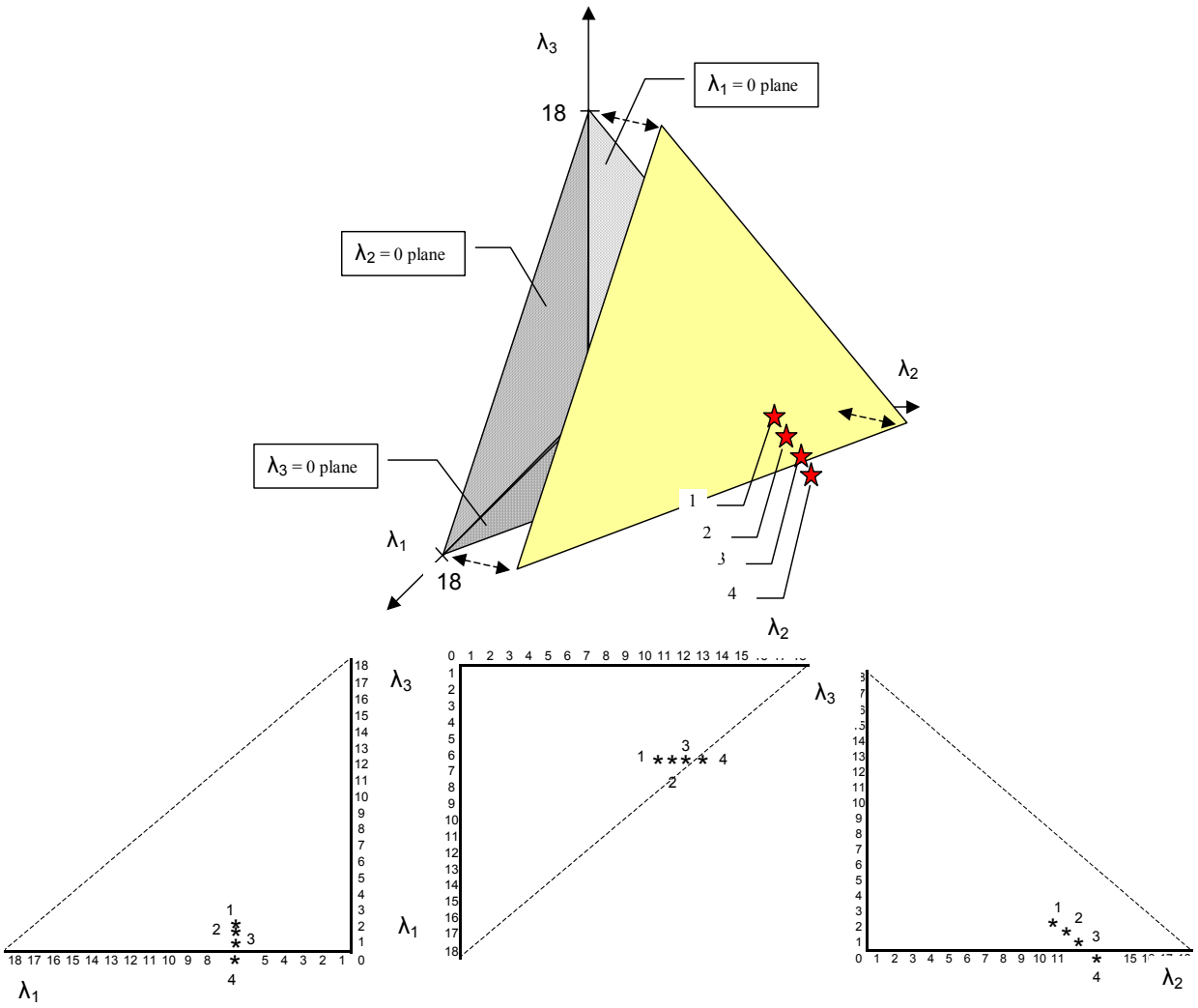

Fig.6: Eigenvalue Space for the Four 3-Link Kinematic Systems - (3,3), (3,2), (3,1), (3,0) using System Eigenvalues as the Co-ordinates of the Four System Points in the Space

Fig.7 shows the eigenvector rotations for the systems shown in Fig.5.

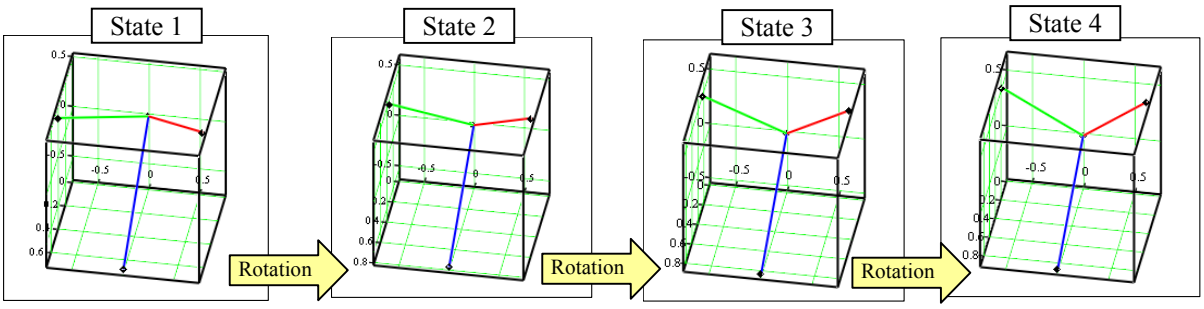

Fig.7: Eigenvector Rotation for Degradation through a Sequence of Faults of a 3-Link Serial System with two 3-dof Joints

Graph Theory may be used to represent the evolution of a kinematic system from its nominal operational state through various sequences of possible kinematic fault states. The collection of all possible 'fault paths' for a particular system, may be represented as a **digraph** [6] of fault states. In contrast to the interchange graph, considered earlier, where vertices and edges represent kinematic links and joints, respectively, this fault-path digraph now has vertices

representing the particular kinematic fault states, and edges representing the transitions between adjacent states. Fault states fall into the following categories, not all of which will occur in every digraph:

- **nominal state** – the unfailed, start state,
- **substitute operational state** – a fault state which still leaves the system with some usable degree of its original mobility
- **non-operational state** – a fault state in which the system ceases to operate
- **intermediate enabling state** – a non-operational fault state, into which a system can be placed by choice, which can be used as an intermediate step in moving to an alternative fault state.
- **non-operational absorbing state** – a terminal condition in which the system ceases to operate, and from which there is no recovery – ie a failure state.

A primary objective is to establish the desirable reconfigurations of a kinematic system by improving the availability of substitute operational states and any associated intermediate enabling states such that the non-operational absorbing state is not reached until the latest possible moment. Consider the 3-link kinematic system on the right hand side of Fig.2. This has 16 possible kinematic fault states obtained by having in various combinations 0, 1, 2 or 3 dof in the joints on either side of the central link. This is represented in digraph form in Fig.8.

The Constraints Matrices, the eigenvalues and the eigenvectors of the sixteen kinematic fault states shown in Fig.8 are listed in Table 2. If a path is traversed through Table 2 via any sequence of kinematic system states from left to right, or from top to bottom, this represents a fault path that can arise as the system progressively loses degrees-of-freedom. Conversely, a path drawn through a sequence of states from right to left, or from bottom to top represents a path that cannot be achieved without some form of intervention to reinstate lost degrees-of-freedom. Table 2 shows that:

- When moving from *left to right* across Table 2, there is an *anti-clockwise* rotation of the eigenvectors about the *y*-axis in the 3D eigenvector space. Y
- When moving from *top to bottom* in Table 2, there is a *clockwise* rotation of the eigenvectors about the *y*-axis in the 3D eigenvector space. Y
- When moving from *right to left* across Table 2, there is a *clockwise* rotation of the eigenvectors about the *y*-axis in the 3D eigenvector space. Y
- When moving from *bottom to top* in Table 2, there is an *anti-clockwise* rotation of the eigenvectors about the *y*-axis in the 3D eigenvector space. Y
- For each of the above four cases, in the 3D eigenvalue space, the point $(\lambda_1, \lambda_2, \lambda_3)$ progresses along the straight line formed by the intersection of the plane $\lambda_1 + \lambda_2 + \lambda_3 = 18$ with the plane $\lambda_1 = 6$.
- All four of the systems (3,3), (2,2), (1,1) and (0,0) have the same three eigenvectors but their second and third eigenvalues differ.
- Systems (3,0) and (0,3) have the same eigenvalues but different eigenvectors, as do systems (2,0) and (0,2), systems (1,0) and (0,1), systems (3,2) and (2,3), systems (3,1) and (1,3), and systems (2,1) and (1,2). Each pair of these 'mirror image' systems exhibits a corresponding mirroring in the *x*- and *z*-components of their eigenvectors.

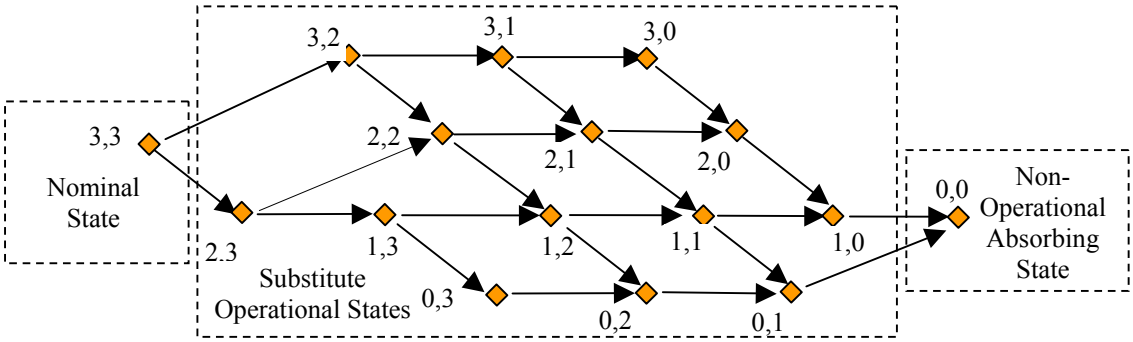

Fig.8: Digraph for the Sixteen Kinematic Fault States of a (3,3) Kinematic System

Table 2: Eigenvalue and (Normalised) Eigenvector Data for the Set of 3-Link Serial Kinematic Systems with Spherical or Planar Joints (an example fault path is overlaid)

3-Link serial kinematic systems (*n*,*m*) [*n* = left joint dof; *m* = right joint dof]				
	(3,3)	**(3,2)**	**(3,1)**	**(3,0)**
Constraints Matrix	$\begin{pmatrix} 6 & 3 & 0 \\ 3 & 6 & 3 \\ 0 & 3 & 6 \end{pmatrix}$	$\begin{pmatrix} 6 & 3 & 0 \\ 3 & 6 & 4 \\ 0 & 4 & 6 \end{pmatrix}$	$\begin{pmatrix} 6 & 3 & 0 \\ 3 & 6 & 5 \\ 0 & 5 & 6 \end{pmatrix}$	$\begin{pmatrix} 6 & 3 & 0 \\ 3 & 6 & 6 \\ 0 & 6 & 6 \end{pmatrix}$
First Eigenvalue	$\lambda_1 = 6$	$\lambda_1 = 6$	$\lambda_1 = 6$	$\lambda_1 = 6$
First Eigenvector	(0.707, 0, -0.707)	(0.800, 0, -0.600)	(0.857, 0, -0.514)	(0.894, 0, -0.447)
Second Eigenvalue	$\lambda_2 = 10.243$	$\lambda_2 = 11$	$\lambda_2 = 11.831$	$\lambda_2 = 12.708$
Second Eigenvector	(0.500, 0.707, 0.500)	(0.424, 0.707, 0.566)	(0.364, 0.707, 0.606)	(0.316, 0.707, 0.632)
Third Eigenvalue	$\lambda_3 = 1.757$	$\lambda_3 = 1$	$\lambda_3 = 0.169$	$\lambda_3 = -0.708$
Third Eigenvector	(0.500, -0.707, 0.500)	(0.424, -0.707, 0.566)	(0.364, -0.707, 0.606)	(0.316, -0.707, 0.632)
	(2,3)	**(2,2)**	**(2,1)**	**(2,0)**
Constraints Matrix	$\begin{pmatrix} 6 & 4 & 0 \\ 4 & 6 & 3 \\ 0 & 3 & 6 \end{pmatrix}$	$\begin{pmatrix} 6 & 4 & 0 \\ 4 & 6 & 4 \\ 0 & 4 & 6 \end{pmatrix}$	$\begin{pmatrix} 6 & 4 & 0 \\ 4 & 6 & 5 \\ 0 & 5 & 6 \end{pmatrix}$	$\begin{pmatrix} 6 & 4 & 0 \\ 4 & 6 & 6 \\ 0 & 6 & 6 \end{pmatrix}$
First Eigenvalue	$\lambda_1 = 6$	$\lambda_1 = 6$	$\lambda_1 = 6$	$\lambda_1 = 6$
First Eigenvector	(0.600, 0, -0.800)	(0.707, 0, -0.707)	(0.781, 0, -0.625)	(0.832, 0, -0.555)
Second Eigenvalue	$\lambda_2 = 11$	$\lambda_2 = 11.657$	$\lambda_2 = 12.403$	$\lambda_2 = 13.211$
Second Eigenvector	(0.566, 0.707, 0.424)	(0.500, 0.707, 0.500)	(0.442, 0.707, 0.552)	(0.392, 0.707, 0.588)
Third Eigenvalue	$\lambda_3 = 1$	$\lambda_3 = 0.343$	$\lambda_3 = -0.403$	$\lambda_3 = -1.211$
Third Eigenvector	(0.566, -0.707, 0.424)	(0.500, -0.707, 0.500)	(0.442, -0.707, 0.552)	(0.392, -0.707, 0.588)
	(1,3)	**(1,2)**	**(1,1)**	**(1,0)**
Constraints Matrix	$\begin{pmatrix} 6 & 5 & 0 \\ 5 & 6 & 3 \\ 0 & 3 & 6 \end{pmatrix}$	$\begin{pmatrix} 6 & 5 & 0 \\ 5 & 6 & 4 \\ 0 & 4 & 6 \end{pmatrix}$	$\begin{pmatrix} 6 & 5 & 0 \\ 5 & 6 & 5 \\ 0 & 5 & 6 \end{pmatrix}$	$\begin{pmatrix} 6 & 5 & 0 \\ 5 & 6 & 6 \\ 0 & 6 & 6 \end{pmatrix}$
First Eigenvalue	$\lambda_1 = 6$	$\lambda_1 = 6$	$\lambda_1 = 6$	$\lambda_1 = 6$
First Eigenvector	(0.514, 0, -0.857)	(0.625, 0, -0.781)	(0.707, 0, -0.707)	(0.768, 0, -0.640)
Second Eigenvalue	$\lambda_2 = 11.831$	$\lambda_2 = 12.403$	$\lambda_2 = 13.071$	$\lambda_2 = 13.810$
Second Eigenvector	(0.606, 0.707, 0.364)	(0.552, 0.707, 0.442)	(0.500, 0.707, 0.500)	(0.452, 0.707, 0.543)
Third Eigenvalue	$\lambda_3 = 0.169$	$\lambda_3 = -0.403$	$\lambda_3 = -1.071$	$\lambda_3 = -1.810$
Third Eigenvector	(0.606, -0.707, 0.364)	(0.552, -0.707, 0.442)	(0.500, -0.707, 0.500)	(0.452, -0.707, 0.543)
	(0,3)	**(0,2)**	**(0,1)**	**(0,0)**
Constraints Matrix	$\begin{pmatrix} 6 & 6 & 0 \\ 6 & 6 & 3 \\ 0 & 3 & 6 \end{pmatrix}$	$\begin{pmatrix} 6 & 6 & 0 \\ 6 & 6 & 4 \\ 0 & 4 & 6 \end{pmatrix}$	$\begin{pmatrix} 6 & 6 & 0 \\ 6 & 6 & 5 \\ 0 & 5 & 6 \end{pmatrix}$	$\begin{pmatrix} 6 & 6 & 0 \\ 6 & 6 & 6 \\ 0 & 6 & 6 \end{pmatrix}$
First Eigenvalue	$\lambda_1 = 6$	$\lambda_1 = 6$	$\lambda_1 = 6$	$\lambda_1 = 6$
First Eigenvector	(0.447, 0, -0.894)	(0.555, 0, -0.832)	(0.640, 0, -0.768)	(0.707, 0, -0.707)
Second Eigenvalue	$\lambda_2 = 12.708$	$\lambda_2 = 13.211$	$\lambda_2 = 13.810$	$\lambda_2 = 14.485$
Second Eigenvector	(0.632, 0.707, 0.316)	(0.588, 0.707, 0.392)	(0.543, 0.707, 0.452)	(0.500, 0.707, 0.500)
Third Eigenvalue	$\lambda_3 = -0.708$	$\lambda_3 = -1.211$	$\lambda_3 = -1.810$	$\lambda_3 = -2.485$
Third Eigenvector	(0.632, -0.707, 0.316)	(0.588, -0.707, 0.392)	(0.543, -0.707, 0.452)	(0.500, -0.707, 0.500)

The example fault path shown overlaid in Table 2 may be represented on the fault-path digraph of Fig.8 as shown overlaid in Fig.9. It can be seen that the clockwise rotated element (from (1,1) to (1,2)) corresponds to a movement opposing system degradation.

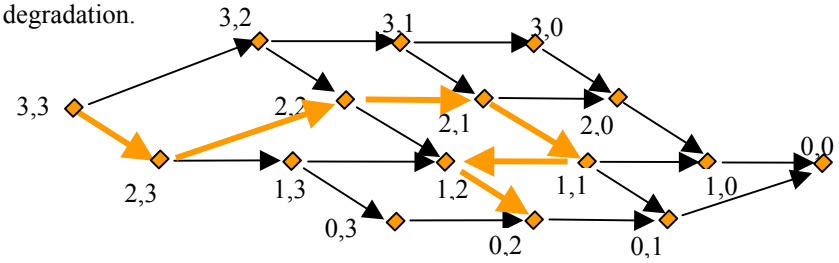

Fig.9: Example Fault Path Overlaid on the Digraph for the Sixteen Kinematic Fault States of a (3,3) Serial Kinematic System

DISCUSSION

Thus, initial indications are that there is potential for the degradation of a kinematic system due to faults, and the effect of any subsequent rectification action, to be represented in terms of Constraints Matrix eigenvalue and eigenvector behaviour. Here, this effect has only been explored in depth for a 3D eigenspace. The behaviour of serial kinematic systems consisting of more than three links and their representations in 4D, 5D, and *n*-D eigenspace, together with that of branched and looped kinematic systems, remains to be explored in detail. This is complicated by the fact that the concept of rotation in higher dimensional spaces is not a straightforward extension of the 2D and 3D situations. Various different 'types' of rotation emerge from 4D onwards, involving fixed planes and hyperplanes, for instance, instead of just fixed points (rotation centres) and fixed lines (rotation axes).

The intention now is to progressively explore these more complex scenarios, and to produce a series of papers which it is hoped will eventually enable the creation of a novel modelling methodology providing a different view of kinematic behaviour from that afforded by current techniques.

CONCLUSION

A Graph Theoretical analysis provides a representation of some aspects of kinematic system reliability and robustness. The examples used here have been relatively simple ones so that the key features of the approach can be easily discussed. However, the Graph Theoretical treatment described is applicable to any manipulator system, and also, in particular, to planetary exploration vehicle locomotion sub-systems.

In practice, even comparatively small (in terms of numbers of links and joints) kinematic systems generate large adjacency matrices and constraints matrices (with correspondingly large determinants), whose analysis and expansion must (realistically) be automated and computerised.

In order for the approach to yield significant benefit, the kinematic systems under consideration need also to embody the necessary clutch / declutch mechanisms to permit the connection / disconnection of joints, so that some states may be utilised for partial recovery from faults, and so that the number of available paths to recovery may be optimised. Typical systems that might exhibit such a capability are: the Mobile Servicing System (MSS) of the International Space Station (ISS); the Space Station Remote Manipulator System (SSRMS – 'Canadarm 2'); the Mobile Remote Servicer Base System (MBS); and the Special Purpose Dextrous Manipulator (SPDM – 'Dextre') elements of the MSS. Each of these embodies the necessary grapple capabilities to allow system reconfigurations [8]. Additionally, the basic functionality of the SSRMS incorporates the ability for sub-elements of the arm to be locked or otherwise controlled in order to enable particular behaviours. Thus, the necessary physical capabilities to reproduce in reality fault-robust strategies developed using the analysis introduced in the previous sections already exist.

REFERENCES

1. Allenby R B J T, *Linear Algebra*, Butterworth Heinemann 'Modular Mathematics Series', 1995.
2. Earl C.F., Rooney J., "Some Kinematic Structures for Robot Manipulator Designs", ASME Journal of Mechanisms, Transmission and Automation in Design, Vol.105, March 1983.
3. Reuleaux F, *The Kinematics of Machinery*, Dover Publications, New York, 1963
4. Rooney J, Open University, "Design 2 - Kinematic Design", Open University text for Mathematics and Computing Technology Third Level Course MT 365 'Graphs, Networks and Design', ISBN 0 7492 2217 4, 1995.
5. Stephenson G, *Mathematical Methods for Science Students, 2nd Ed*., 1973, Pearson Prentice Hall, ISBN 0-582-44416-0
6. Wilson RJ, *Introduction to Graph Theory*, 4th. Ed., Longman, 1996, ISBN 0-582-24993-7
7. Yan H.S., Hall A.S. "Linkage Characteristic Polynomials: Definitions, Coefficients by Inspection", American Society of Mechanical Engineers (ASME) Journal, Vol.103, July 1981
8. Web: http://en.wikipedia.org/wiki/Canadarm2, accessed 26 August 2008
9. Web: http://www.scienceray.com/Technology/Space Robot—Dextre 129460, accessed 19 August 2008
10. Web: http://en.wikipedia.org/wiki/Flight_simulator, accessed 26 August 2008